Phase relations in the Ba–Y–Cu–O films on $SrTiO_3$ for the *ex situ* BaF_2 process

W. Wong-Ng,[a] I. Levin, M. Otani, M. D. Vaudin, L. P. Cook, and J. Cline
Ceramics Division, National Institute of Standards and Technology, Gaithersburg, Maryland 20899

R. Feenstra
Materials Science and Technology Division, Oak Ridge National Laboratory, Oak Ridge, Tennessee 37831

T. Holesinger
Materials Science and Technology, Los Alamos National Laboratory, Los Alamos, New Mexico 87545

(Received 23 December 2006; accepted 6 February 2007; published online 9 March 2007)

In situ x-ray diffraction was used to establish the phase relations in high-T_c superconductor Ba–Y–Cu–O films grown on $SrTiO_3$ through the *ex situ* BaF_2 process. These relations differ from bulk equilibrium phase assemblages in the $BaO-Y_2O_3-CuO_x$ system. In particular, BaY_2CuO_5 (the "green phase"), a common impurity phase in bulk processing, is absent in the films. Because of the absence of this green phase, the compositional stability field of $Ba_2YCu_3O_{6+x}$ expands considerably as compared to that of the bulk system, resulting in the tie lines $Ba_2YCu_3O_{6+x}-Y_2O_3$ and $Ba_2YCu_3O_{6+x}-Y_2Cu_2O_5$. © *2007 American Institute of Physics*. [DOI: 10.1063/1.2713124]

Energy shortages and electricity outages present serious global problems with an ever-increasing demand for reliable grids and additional energy sources. High-temperature superconductors have demonstrated potentials for improvement in the electrical distribution grids and efficient utilization of energy sources. Research and development of coated conductors for wire/tape applications at an accelerated pace are deemed important for meeting the national and international energy needs.

Ion beam assisted deposition[1,2] and rolling assisted biaxially textured substrate[3–5] (RABiTS) are the two state-of-the-art technologies to produce biaxially textured substrates for coated conductor applications. Coated conductors are based on $Ba_2YCu_3O_{6+x}$ (Y-213) and $Ba_2RCu_3O_{6+x}$ (*R*-213, *R* =lanthanides) as the principal superconducting materials. These conductors incorporate a metallic substrate and buffer multilayers separating the substrate and the superconductor film. The buffer layers serve as physical/chemical barriers and provide a template for a highly textured growth of the superconductor layer. Examples of two suitable buffer layers immediately underneath the superconductor layer include CeO_2 and $SrTiO_3$.

Manufacturing of long-length coated conductors faces significant technological challenges. The *ex situ* BaF_2 process[3–13] has been considered as one of the feasible processes for producing high-quality long-length coated conductors. In this approach, films were prepared using either the fast rate e-beam deposition or trifluoroacetate solution technique[13] followed by high-temperature heat treatment in the presence of water vapor under a reduced oxygen pressure atmosphere. The *ex situ* annealing typically takes place between 725 and 800 °C.

Phase equilibrium diagrams provide roadmaps for coated conductor processing and for the understanding of their high-T_c properties. Currently, bulk phase relations[14–18] are used as references for the Ba–Y–Cu–O superconductor film processing. However, phase assemblages in thin films can differ from those predicted by the bulk phase equilibria; therefore, understanding of phase relations for the $BaO-Y_2O_3-CuO_x$ thin films on CeO_2 and $SrTiO_3$ substrates is critical for the development of coated conductors.

In this study, seven films with compositions in the $BaCuO_{2+x}-Y_2O_3-CuO_x$ region were prepared using the *ex situ* BaF_2 process [Table I and Fig. 1; the phase relations shown in Fig. 1 correspond to the equilibrium conditions of 100 Pa p_{O_2} (0.1% O_2 by volume) and 810 °C, and the bulk samples were prepared using high-temperature solid-state techniques[14]]. Precursor films were prepared by electron-beam evaporation of Cu metal, Y metal, and BaF_2 in a stainless steel vacuum chamber at room temperature on $SrTiO_3$ substrates.[10] The substrates were annealed at 1000 °C in 0.1 MPa of O_2 prior to the precursor deposition. During evaporation, the source materials Cu, Y, and BaF_2 were contained in removable tantalum crucibles and were placed inside the hearths of the e-beam guns. All films were deposited on (100) single crystal $SrTiO_3$ substrates. The film compositions were derived from the evaporation rate monitor readings, which were calibrated using Rutherford backscattering and inductively coupled plasma analysis. The precursor (BaF_2+Cu+Y) films were relatively stable in air; yet, as a precaution, the films were kept in a dry box.

A high-temperature Siemens D5000 θ-θ x-ray diffractometer[19] equipped with a position sensitive detector and a high-temperature furnace was modified by adding a gas flow apparatus. This apparatus includes a series of bubblers containing NaCl-saturated water at room temperature ($p_{H_2O} \approx 2.1$ kPa or 0.021 atm, at $T=22$ °C) and an oxygen analyzer. Helium gas containing ≈100 Pa O_2 (≈0.1% O_2 by volume) was flowed through the bubblers and passed directly over the film surface. Cu $K\alpha$ radiation was used. The diffraction patterns (about 8 min long each) were recorded every 50 °C upon heating to 735 °C and then continuously upon the exposure at this temperature. Among the seven films, three (Films 1, 3, and 6) were studied using high-temperature x-ray diffraction (HTXRD). The other four were annealed in an atmospherically controlled box furnace under the pres-

[a]Electronic mail: winnie.wong-ng@nist.gov

TABLE I. Seven compositions prepared in the $BaO-Y_2O_3-CuO_x$ system for this study.

Film	Ba	Y	Cu	Stoichiometry	phases present on film (735 °C)
1	25	50	25	(BaY_2CuO_x)	$Ba_2YCu_3O_{6+x}$, Y_2O_3 (main phases)
2	42.5	10	47.5		$Ba_2YCu_3O_{6+x}$, $BaCuO_{2+x}$ (main phases)
3	31.0	22.5	46.5	$(Ba_2Y_{1.45}Cu_3O_x)$	$Ba_2YCu_3O_{6+x}$, Y_2O_3
4	30.4	17.4	52.2	$(Ba_{1.5}Y_{1.05}Cu_3O_x)$	$Ba_2YCu_3O_{6+x}$, $Y_2Cu_2O_5$, CuO
5	27.4	26.0	46.6	$(Ba_2Y_{1.9}Cu_{3.4}O_x)$	$Ba_2YCu_3O_{6+x}$, $Y_2Cu_2O_5$, Y_2O_3
6	29.9	14.8	55.3	$(Ba_2Y_1Cu_{3.7}O_x)$	$Ba_2YCu_3O_{6+x}$, CuO, $BaCuO_{2+x}$ (small)
7	29.7	25.7	44.6	$(Ba_2Y_{1.73}Cu_3O_x)$	$Ba_2YCu_3O_{6+x}$, $Y_2Cu_2O_5$, Y_2O_3

ence of water vapor at 735 °C for about 4 h and then characterized *ex situ* using x-ray diffraction in a conventional θ-2θ powder diffractometer. The phase assemblages that are present in these films are summarized in Table I.

Figures 2 and 3 show the HTXRD patterns for film 1 having a composition Ba:Y:Cu=1:2:1 that corresponds to the "green phase." Between 500 and 600 °C, the formation of barium oxyfluoride, $Ba(F_{2-2x}\square_x)O_x$ ($\square$ represents a vacant site), and Y_2O_3 occurred. $Ba(F_{2-2x}\square_x)O_x$ crystallizes with a superstructure that was attributed to the anion ordering in the cubic BaF_2-like barium oxyfluoride phase.[17] The reflections of this phase are indexable using a monoclinic unit cell with $a \approx 7.20$ Å ($a_{BF}\sqrt{6}/2$), $b \approx 4.38$ Å ($a_{BF}/\sqrt{2}$), $c \approx 10.85$ Å ($a_{BF}\sqrt{3}$), and $\beta \approx 92°$ (where subscript BF refers to the cubic BaF_2). This phase disappears after about 1 h exposure at 735 °C. In contrast, the Y_2O_3 phase persists throughout the entire annealing cycle. The Y-213 phase first forms at 735 °C and continues to grow with increasing annealing time. The final phase assemblage consists primarily of a mixture of Y-213 and Y_2O_3. No green phase was observed in film 1 even after prolonged annealing at 735 °C.

Similarly, no green phase was detected in film 3 upon the completion of the *in situ* HTXRD experiments (Fig. 4). In this film, both $Ba(F_{2-2x}\square_x)O_x$ (Ref. 17) and $Y_2Cu_2O_5$ phases appear briefly but vanish completely after an ≈90 min exposure at 735 °C. The Y-213 that begins to form at about 700 °C continues to grow and remains stable. Y_2O_3 forms after ≈60 min at 735 °C and remains in the film even after a continuing annealing for 2 h. Therefore, the composition of film 3 was concluded to reside on the tie line between Y-213 and Y_2O_3 instead of the three-phase region $Y_2O_3-BaY_2CuO_5-CuO_x$ (Fig. 1). We propose that $Ba(F_{2-2x}\square_x)O_x$ reacts with $Y_2Cu_2O_5$ and H_2O vapor to form Y-213, Y_2O_3, and HF(g).

Ex situ x-ray powder diffraction for film 4 ($Ba_{1.5}Y_{1.05}Cu_3O_x$), that was annealed at 735 °C for ≈4 h revealed a mixture of $Y_2Cu_2O_5$, Y-213, and CuO. This result suggests the compatibility of Y-213 with $Y_2Cu_2O_5$ rather than with the green phase. *Ex situ* studies of film 5 ($Ba_2Y_{1.9}Cu_{3.4}O_x$) confirm the compatibility of $Y_2Cu_2O_5$, Y-213, and Y_2O_3 which was suggested by the *in situ* HTXRD. These conclusions were further corroborated by the transmission electron microscopy (TEM) study of a film of composition $Ba_2Y_{1.7}Cu_3O_x$ (composition corresponds closely to that of film 7). The bright field image of the upper half of this film (Fig. 5) shows inclusions of both Y_2O_3 and $Y_2Cu_2O_5$ in addition to the major Y-213 phase. Most of the inclusion particles in the inner half of the film were found to be $Y_2Cu_2O_5$. No green phase was detected in this sample by TEM.

In summary, phase relations for the thin films having CuO-rich compositions in the vicinity of Y-213 (Fig. 6), which were prepared using a BaF_2 process, differ from those predicted by the bulk phase equilibria (Fig. 1). In particular, in thin films the Y-213 phase is compatible with Y_2CuO_5 and Y_2O_3, whereas BaY_2CuO_5 is absent. Because of the absence of this green phase, the compositional stability field of $Ba_2YCu_3O_{6+x}$ expands considerably as compared to that of the bulk system, resulting in the tie lines $Ba_2YCu_3O_{6+x}-Y_2O_3$ and $Ba_2YCu_3O_{6+x}-Y_2Cu_2O_5$. These results highlight the need for investigation of phase relations in thin films under the actual processing conditions.

Common reasons for different phase relationships in bulk and thin film materials include strain, texturing, and kinetic details that are determined by the substrate, film thickness, and the processing conditions. In the BaF_2 *ex situ* process, the difference could also be due to the presence of

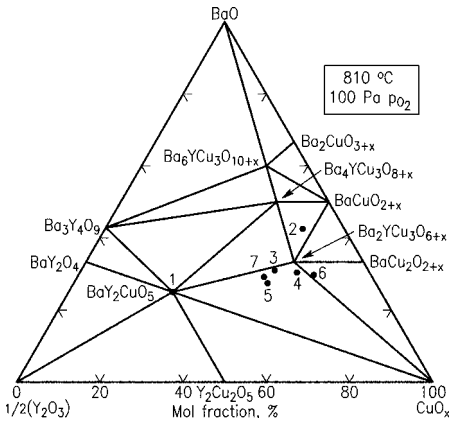

FIG. 1. Phase equilibrium diagram of the bulk system $BaO-Y_2O_3-CuO_x$ at 810 °C and 100 Pa.

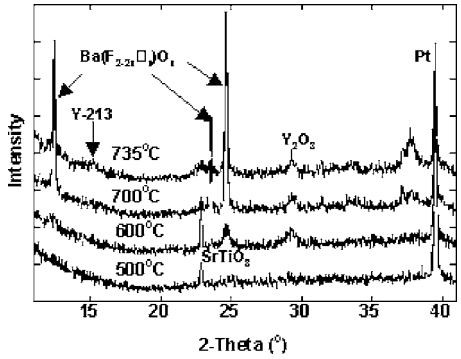

FIG. 2. High-temperature x-ray diffraction patterns of film 1 (Ba:Y:Cu of 1:2:1) as a function of temperature upon heating.

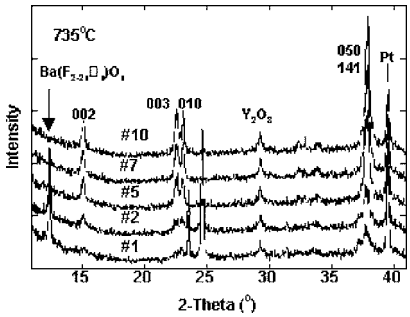

FIG. 3. High-temperature x-ray diffraction patterns of film 1 (Ba:Y:Cu of 1:2:1) as a function of time at 735 °C. The absence of BaY_2CuO_5 phase is illustrated.

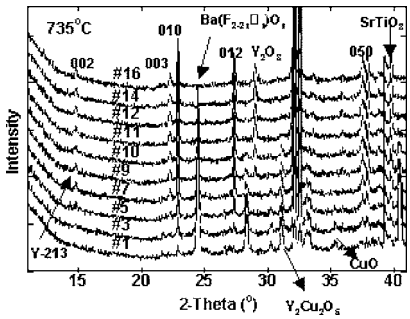

FIG. 4. HTXRD of film 4 annealed at 735 °C as a function of time. The compatibility of Y-213 and Y_2O_3 phase is observed after annealing for 60 min.

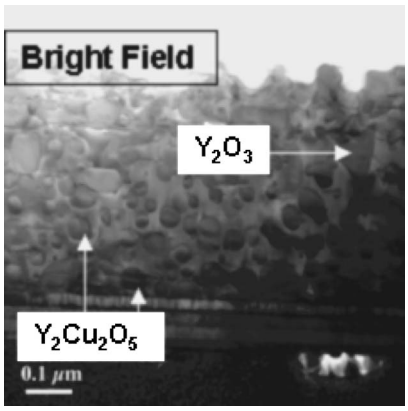

FIG. 5. Bright field TEM image of a 1.1 μm thick Y-rich film on a rolling assisted biaxially textured substrate (RABiTS). The composition ($Ba_2Y_{1.7}Cu_3O_x$) corresponds closely to that of film 7. The film was converted as described in Ref. 10 using a processing temperature of 780 °C and oxygen pressure of 25 Pa. In addition to the $Ba_2YCu_3O_x$ phase, many inclusions of both Y_2O_3 and $Y_2Cu_2O_5$ phases are present throughout the film. Three buffer layers (form top to bottom: CeO_2, Y-stabilized zirconia, and Y_2O_3) are visible below the film.

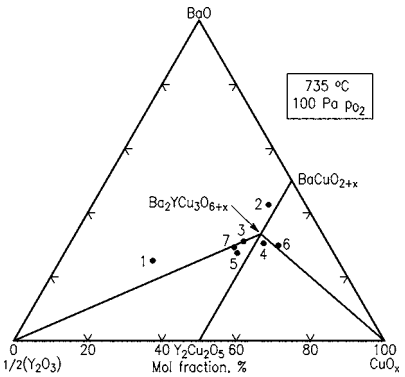

FIG. 6. Thin film phase relations for the CuO- and Y_2O_3-rich regions of the $BaO-Y_2O_3-CuO_x$ system.

fluorine. As the knowledge of phase relations is important for coated conductor processing, we plan to further investigate the causes of these differences by analyzing phase formation in Ba–Y–Cu–O (instead of fluorides) films on $SrTiO_3$ using a high-throughput combinatorial approach.[20] These experiments will determine the effect of fluorine on phase assemblages. The complex phase compatibility in the CuO-deficient region of the diagram will also be addressed in the future work.

The partial financial support from the U.S. Department of Energy is acknowledged. The work at the Oak Ridge National Laboratory was sponsored by the U.S. Department of Energy-Office of Electricity Delivery and Energy Reliability, Superconductivity Program for Electric Power Systems under Contract No. DE-AC05-00OR22725 with Oak Ridge National Laboratory, managed and operated by UT-Battelle, LLC.

[1] S. R. Foltyn, E. J. Peterson, J. Y. Coulter, P. N. Arendt, Q. X. Jia, P. C. Dowden, M. P. Maley, X. D. Wu, and D. E. Peterson, J. Mater. Res. **12**, 2941 (1997).
[2] M. Bauer, R. Semerad, and H. Kinder, IEEE Trans. Appl. Supercond. **9**, 1502 (1999).
[3] M. W. Rupich, W. Zhang, X. Li, T. Kodenkandath, D. T. Verebelyi, U. Schoop, C. Thieme, M. Teplitsky, J. Lynch, N. Nguyen, E. Siegal, J. Scudiere, V. Maroni, K. Venkataraman, D. Miller, and T. G. Holesinger, Physica C **412–414**, 877 (2004).
[4] X. Li, M. W. Rupich, W. Zhang, N. Nguyen, T. Kodenkandath, U. Schoop, D. T. Verebelyi, C. Thieme, M. Jowett, P. N. Arendt, S. R. Foltyn, T. G. Holesinger, T. Aytug, D. K. Christen, and M. P. Paranthaman, Physica C **390**, 249 (2003).
[5] M. Paranthaman, C. Park, X. Cui, A. Goyal, D. F. Lee, P. M. Martin, T. G. Chirayil, D. T. Verebelyi, D. P. Norton, D. K. Christen, and D. M. Kroeger, J. Mater. Res. **15**, 2647 (2000).
[6] P. M. Mankiewich, J. H. Scofield, W. J. Skocpol, R. E. Howard, A. H. Dayem, and E. Good, Appl. Phys. Lett. **51**, 1753 (1987).
[7] S.-W. Chan, B. G. Bagley, L. H. Greene, M. Giroud, W. L. Feldmann, K. R. Jenkin II, and B. J. Wilkins, Appl. Phys. Lett. **53**, 1443 (1988).
[8] R. Feenstra, T. B. Lindemer, J. D. Budai, and M. D. Galloway, J. Appl. Phys. **69**, 6569 (1991).
[9] M. Yoshizumi, M. I. Seleznev, and M. J. Cima, Physica C **403**, 191 (2004).
[10] R. Feenstra, A. A. Gapud, F. A. List, E. D. Specht, D. K. Christen, T. G. Holesinger, and D. M. Feldman, IEEE Trans. Appl. Supercond. **15**, 2803 (2005).
[11] L. Wu, V. F. Solovyov, H. J. Wiesmann, Y. Zhu, and M. Suenaga, Appl. Phys. Lett. **80**, 419 (2002).
[12] W. Wong-Ng, I. Levin, R. Feenstra, L. P. Cook, and M. D. Vaudin, Semicond. Sci. Technol. **17**, S548 (2004).
[13] M. Yoshizumi, I. Seleznev, and M. J. Cima, Physica C **403**, 191 (2004).
[14] W. Wong-Ng, L. P. Cook, and J. Suh, Physica C **377**, 107 (2002).
[15] K. Osamura and W. Zhang, Z. Metallkd. **84**, 522 (1993).
[16] R. S. Roth, C. J. Rawn, F. Beech, J. D. Whitler, and J. O. Anderson, in *Ceramic Superconductors II*. edited by M. F. Yan (American Ceramic Society, Wersterville, OH, 1988), P. B.
[17] W. Wong-Ng, I. Levin, L. P. Cook, and R. Feenstra, Appl. Phys. Lett. **88**, 103507 (2006).
[18] B. T. Ahn, V. Y. Lee, R. Beyers, T. M. Gür, and R. A. Huggins, Physica C **167**, 529 (1990).
[19] Certain commercial equipment, instruments, or materials are identified in this letter to foster understanding. Such identification does not imply recommendation or endorsement by the National Institute of Standards and Technology, nor does it imply that the materials or equipment identified are necessarily the best available for the purpose.
[20] H. Koinuma and I. Takeuchi, Nat. Mater. **3**, 429 (2004).